JBIS, Vol. 62, pp.342-353, 2009

FEASIBILITY OF 20 KM FREE-STANDING INFLATABLE SPACE TOWER

R.K. SETH[1*], B.M. QUINE[1,2] AND Z.H. ZHU[2]
1. *Department of Physics and Astronomy, York University.*
2. *Department of Earth and Space Science and Engineering, York University, 4700 Keele Street, Toronto, Ontario, Canada M3J 1P3.*

Email: rajseth@yorku.ca*

This paper describes the theory and analysis for the construction of a thin walled inflatable space tower of 20 km vertical extent in an equatorial location on Earth using gas pressure. The suborbital tower of 20 km height would provide an ideal surface mounting point where the geosynchronous orbital space tether could be attached without experiencing the atmospheric turbulence and weathering in the lower atmosphere. Kevlar is chosen as an example material in most of the computations due to its compatibility in the space environment. The Euler beam theory is employed to the inflatable cylindrical beam structure. The critical wrinkling moment of the inflated beam and the lateral wind load moments are taken into account as the key factors for design guidelines. A comparison between single inflatable cylindrical beam and inflatable multiple-beam structures is also presented in order to consider the problems involving control, repair and stability of the inflated space tower. For enhancing load bearing capacity of the tower and for availability of more surface area at the top, the non-tapered inflatable structure design is chosen for the basic analysis, however further analysis can be performed with tapered structures.

Keywords: Space tower, inflatable beam, cylindrical, inflatable multi-beam structure

1. INTRODUCTION

One of the most demanding current mega engineering projects on Earth is to build a space elevator for various space applications. The current trend in new inflatable structure applications lends itself to study for the preliminary engineering design analysis of the space tower. Today, to access outer space, conventional chemical rockets are the only method in use. This method is extremely inefficient since a sizeable amount of energy is consumed during the flight to overcome the depth of the gravity potential energy well and to overcome atmospheric drag. As a result, launch costs per kilogramme of the payloads are very high from Earth to Low Earth Orbit (LEO). For applications involving the extensive utilization of space such as space colonization, much cheaper and efficient launch methods are required. The space tower, one of the alternatives to conventional chemical rockets, is proposed as an efficient means to access space with reduced environmental damage to the atmosphere. A tower can be utilized as a launching station at a sufficient altitude for space flight to occur. The work done is significantly less because the losses due to atmospheric drag and propulsive efficiency are almost eliminated by using a space elevator system. The transport system for the space tower could comprise electrically powered cabins carrying payloads and tourists vertically along the length of the tower. Fixed observatories can be installed at different altitudes along the stations in the near-space environment. These fixed stations, provided at different heights, would be advantageous being closer and fixed to Earth compared to geostationary systems.

With the advent of modern materials, it is possible now to design towers many kilometres in height. However, conventional towers of only 1/2 km in vertical extent are very expensive, costing tens of billions of dollars. In comparison, the proposed 20 km tower using inflatable technology would be much more cost effective since it would need approximately the same amount of money. Inflatable structures are one of the emerging technologies that can potentially revolutionize the design of space tower structures. Compared to conventional structures, inflatable structures have several distinct advantages, such as being light-weight, having lower life cycle costs, and a simpler design with fewer parts [1].

An inflatable tower can be built to any height by making its base sufficiently large. Usually, the base of an inflatable tower is not large compared to its height. The tower beam made of new fabric materials can be inflated with air, helium and hydrogen. Unfortunately, hydrogen is dangerous and its utility as a pressurized gas may be limited below 10 km.

2. BACKGROUND

Towers are tall "artificial"structures built to take advantage of their height and can stand alone or as part of a larger structure. Towers have been used by mankind since ancient times [2]. The Book of Genesis refers to an idea of "stairway to heavens" and includes Tower of Babel and Jacob's Ladder. In nineteenth century, the concept of space elevator was proposed by K.E. Tsiolkovski, a school teacher in St. Petersburg, Russia, in his manuscript "*Speculation about Earth and Sky and on Vesta*,"[3]. He provided a "thought experiment" on a tower into space. The concept was rediscovered by the American engineer, Jerome Pearson, in the early 1970s. Pearson provided a physical basis for the construction of a space tower and his idea published in 1975 [4]. Novelist Sir Arthur Clarke consulted with Pearson when writing his novel, "*The Fountains of Paradise*" [5]. The novel publication brought Pearson's idea of the space elevator to wide population audience in 1978.

The construction of an inexpensive inflatable suborbital space tower between 3 and 100 km height has also been proposed by Bolonkin [6]. Recently, a guided stabilised tower approach has been proposed by authors for the construction of suborbital inflatable towers to access altitudes above 20 km that is realisable utilising current material technologies. The proposed structure comprised of pneumatically inflated sections that are actively controlled and stabilised by using gyro-control machinery to balance external disturbances and support the structure [7].

3. MATERIAL SELECTION

Current industry widely produces artificial fibres having tensile strength σ up to 6.08 *GPa*, (σ = 620 kg/mm^2) and density ρ = 1800 kg/m^3 [6]. Kevlar 49 with a tensile strength σ = 3.6 *GPa* and density ρ = 1440 kg/m^3 is selected as an example material for most of the computation and analysis here due to its suitable mechanical properties to the inflatable beam structures in space environment. The other fabrics can also be chosen to further elaborate the analysis. Among the man-made fibres, the organic fibre Kevlar is a highly flexible composite with high strength, low cost and impact resistance. Past space structures have already utilized Kevlar as a design material. On May 20, 1996, the space shuttle STS-77 mission successfully deployed an inflatable antenna, called Spartan. The experiment was intended to demonstrate the maturity of the inflatable technology. The torus and struts were made of 0.3 mm thick Kevlar with Neoprene coating. The cost of the whole experiment was in the order of $10 million [8, 9]. The experiment of the inflatable antenna proved to be very valuable for inflatable technology in space engineering. The inflated structure is subject to possible punctures caused by high velocity space debris. However, the high tensile strength of Kevlar resists punctures. The interwoven design of Kevlar resists ripping, tearing, and cracking [10].

Today, there are three standard grades of Kevlar available: Kevlar 29, Kevlar 49, and Kevlar 149. Among them, Kevlar 49 is dominant in structural composites because of its higher modulus. Kevlar 29 is used in composites when higher toughness, damage tolerance, or ballistic stopping performance is desired. An ultra-high-modulus fibre, Kevlar 149, is also available. Table 1 shows the mechanical properties of Kevlar for the different grades [11-13].

Recently, Carbon nanotube technology (CNT) has developed rapidly. CNTs are a new form of carbon, formed in laboratories and are not commercially available on the scale required for constructing a space elevator. However, the strength of CNT combined with its low density makes these materials important when considering the design of a space elevator. If CNTs prove to be suitable for mass manufacturing, this may be an ideal material for the construction of a future space elevator. The theoretical density of a pure carbon nanotube is 1300 kg/m^3 and its strength (tensile yield stress) may be as high as 300 GPa, although the NIAC Phase 1 report [14] uses the more conservative value of 130 GPa. Even this more conservative figure is several orders of magnitude higher than the strength of conventional engineering materials and would be ideal for building a space tower. Although CNTs are the strongest material discovered so far, due to its non-availability on mass scale, the material is not taken into account for the current analysis. In contrast, Kevlar 49 is a commercially available material, also found successful in past space missions and is chosen for the analysis here.

The tensile stress σ and density ρ of a material can be used as a basis to estimate overall vertical length (characteristic length l_c) that can be maintained by material of construction of the cylindrical tower of radius R and thickness t.

(σ = *weight of tower material* ($2\pi Rtl_c\rho g$/*Area*($2\pi Rt$)).

The characteristic length for a space tower is given as $\frac{\sigma}{\rho g}$ [15].

Where g is acceleration due to gravity. The length scale depends on the tensile strength and density of the material chosen and varies for different materials.. Using commercially available *Kevlar 49*, (σ = 3.6 *GPa*, ρ = 1440 kg/m^3), an already proven material in past space missions, the characteristic length is found to be *255 km*. For (CNT) carbon fibre (σ = 130 *GPa*, ρ = 1300 kg/m^3), currently available in the laboratory, the value could be as high as *10,200 km*.

4. STRUCTURAL CONCEPT

The tower structure consists of pneumatically pressurized beams. The beams are fabricated using high tensile stress material such as Kevlar. The core structure of a space tower can be designed using multiple-beams inflated by low atomic gas or an air-gas mixture. The advantage of using an inflated multiple-beam structure is that the attitude of the structure can be controlled by differential changes in pressure in different segments of the structure. The active control mechanism can be employed by making use of spinning gyros at specific heights along with the height of the tower [7].

The basic typical core-structure configurations of the tower using pneumatically pressurized multiple-beams are shown in Fig. 1. These possible structural configurations have typical arrangement of pods and segments along the length of the structure as shown. A 7.0 m scale model of a structure similar to Elevator A, installed in a stairwell, is shown in Fig. 2. A minimum pressure of 48,000 Pa (7PSI) is required for its free-standing. The structure consists of three equal-sized inflated beams braced at approximately 1 metre intervals by making use of the brackets. The diameter of each beam is 0.082 m. The

TABLE 1: *Mechanical Properties of Kevlar.*

Grade	Density g/cm^3	Tensile Modulus GPa	Tensile Strength GPa	Tensile Elongation %
29 (High Toughness)	1.44	83	3.6	4.0
49 (High Modulus)	1.44	131	3.6-4.1	2.8
149 (Ultrahigh Modulus)	1.47	179	3.4	2.0

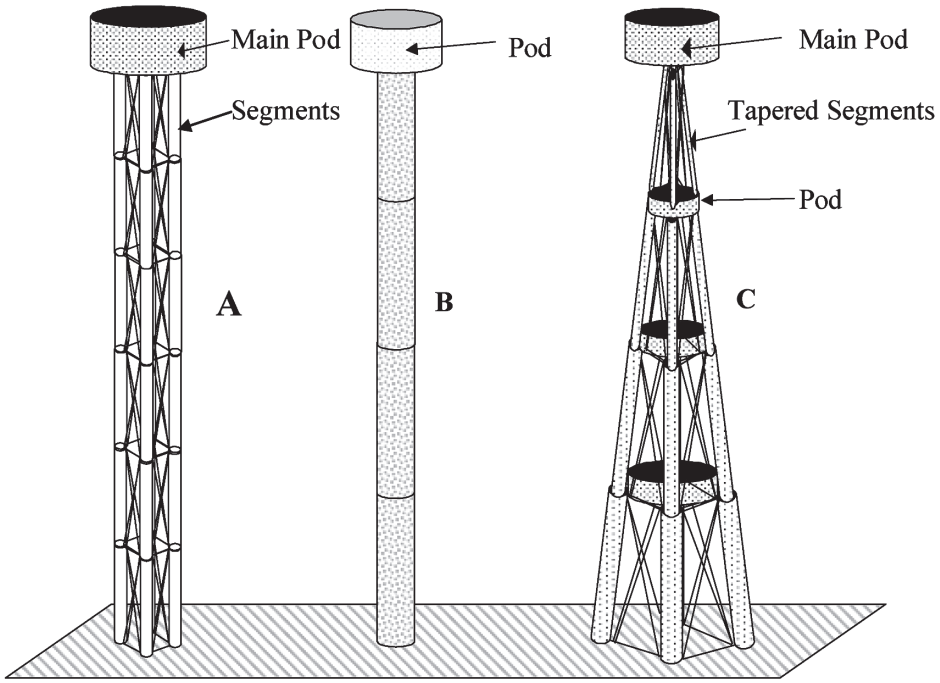

Fig. 1 Core-structure configurations (A, B and C).

overall diameter of the structure is 0.34 m. The beams are fabricated using fibre reinforced polyethylene material with an average thickness of 0.0013 m. The 7.0 m structure deployed vertically in the stairwell has a total mass of 17 kg excluding the heavy base support.

5. THEORY OF INFLATABLE STRUCTURES

The stiffness and load capacity of an inflatable structure depends upon the internal gas pressure. The maximum value of the applied internal gas pressure depends upon the tensile strength of the material and geometrical parameters including the radius and thickness of the structure wall.

When the cylindrical fabric beam is inflated, the material comprising the beam is subjected to pressure loading, and hence stressed in all directions. The stresses resulting from this pressure are typically parameterized as functions of the radius and thickness of the beam element under consideration, the shape of the inflated structure usually, and the applied pressure. The most common method to analyse the inflated cylindrical beam is based on a simple mechanics approach which is applicable to thin wall pressure vessels that have a ratio of inner radius, R, to wall thickness, t, of $R/t \geq 10$ [16]. When an internal gas pressure exists in the inflated cylindrical beam, two types of stresses are generated: axial stress σ_a and hoop stress σ_h, such as [16]:

$$\sigma_a = \frac{pR}{2t}; \quad \sigma_h = \frac{pR}{t} \tag{1}$$

The corresponding maximum gas pressures in the inflatable beam can be obtained as:

$$p_a = \frac{2\sigma t}{R}; \quad p_h = \frac{\sigma t}{R} \tag{2}$$

The value of pressure corresponding to hoop stress p_h is less than that corresponding to axial stress p_a. Therefore, the pressure value corresponding to hoop stress determines the maximum safe limit of the internal gas pressure with an additional safety factor to be applied. Therefore, p_h gives the maximum limiting value of the internal gas pressure corresponding to given R/t ratio as

Fig. 2 A 7 m multi-beam inflated free standing structure designed and installed in a stairwell.

$$p_{\max} = \frac{\sigma}{R/t} \tag{3}$$

It is assumed here that the internal gas pressure is kept constant throughout the entire inflated column of height z. In practice, the value of the air or gas pressure in a column varies with the altitude as follows [6, 7]:

$$p = p_0 e^{\left(\frac{-\mu g z}{R_g T}\right)} \tag{4}$$

where p is the pressure at a height z and p_0 is the pressure at the

planet's surface. R_g is the universal gas constant, μ is the molecular mass, T is the temperature of the air or gas in Kelvin, and g (9.8 $m.sec^{-2}$) is the acceleration due to gravity, respectively. The typical value of the gas constant is R_g = 8.314 $Joule.K^{-1}mol^{-1}$. The typical value of molecular mass for air is $\mu = 28.96*10^{-3}$ $kg.mol^{-1}$ (28.96 $gm.mol^{-1}$), whilst for helium, $\mu = 4*10^{-3}$ $kg.mol^{-1}$ (4 $gm.mol^{-1}$) and for hydrogen $\mu = 2*10^{-3}$ $kg.mol^{-1}$ (2 $gm.mol^{-1}$). To keep the pressure constant in the tower, the whole tower is divided vertically into a number of equal sections as shown in Fig. 3(a). A high pressurized inflated beam using a compressor is also shown in Fig. 3(b). The pressure in all the sections can be kept the same with the help of pressure sensors in each section and by using gas compressors and pressure regulators. If the height of each section is taken in the range 25-100 m, then using Eq. (4), the percentage change in the pressure due to altitude is around 0.3-1.4% for air, 0.04-0.2% for helium and 0.02-0.1% for hydrogen, which is small and therefore may be neglected. Taking the given range of tensile strength, the variation of maximum pressure with R/t ratio is computed using Eq. (3) and is shown in Fig. 4.

The air or gas density varies with the pressure and temperature. At standard temperature and pressure (STP), density for air is ρ_g = 1.29 kg/m^3, for helium ρ_g = 0.1787 kg/m^3 and for hydrogen ρ_g = 0.0898 kg/m^3. The typical average temperature ranging from ground to 20 km atmosphere is *242 K* [17]. The density of air at different pressures and temperatures can be found as

$$\rho_g = \frac{\mu p}{R_g T} \tag{5}$$

Let ρ_g' be the density of the gas at a pressure p'. Therefore the values of the densities of hydrogen, helium and air at different pressures (assuming constant temperature) can be computed using Eq. (5) as

$$\rho_g' = \rho_g \frac{p'}{p} \tag{6}$$

Eq. (6) simply shows that the density of the gas is directly proportional to its pressure. Here p is the pressure at STP and p' is the pressure corresponding to given tensile strength of the material and R/t ratio, see Eq. (3). The Eq. (6) can be written as

$$\rho_g' = \frac{\rho_g}{p}\left(\frac{\sigma}{R/t}\right) \tag{7}$$

And the results of computations by using Eq. (7) for hydrogen, helium and air using Kevlar are shown in Fig. 5.

The inflated cylindrical tower is divided into sections each with the same gas pressure. To determine the value of maximum optimal attainable height, the load of each section and hence of the entire tower due to the presence of internal gas must be taken into account in addition to the weight of the tower. Thus, the maximum attainable height H for particular R/t ratio is given by the equality

$$\pi R^2 p' = 2\pi RtH\rho g + \pi R^2 H\rho_g' g$$

where ρ_g' is the density of the gas/or air to be used at internal gas pressure p'.

Setting the value of $p' = p_{\max}$ from Eq. (3) into the above equation leads to the maximum attainable height of the tower and is given by

$$H_{max} = \frac{\sigma}{2\rho g + \left(\frac{R}{t}\right)\rho_g' g} \tag{8}$$

and Eq. (5) corresponding to density ρ_g' of the gas/or air to be used at internal gas pressure p' becomes

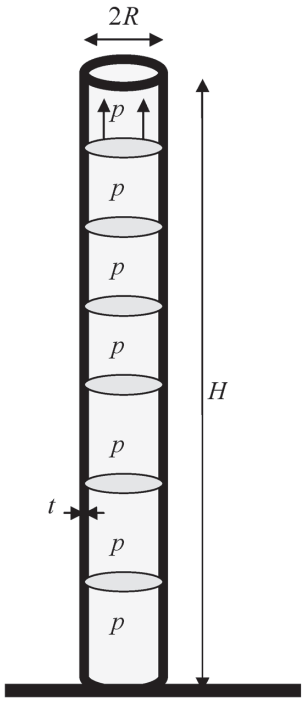

(a)

(b)

Fig. 3 (a) Inflatable non-tapered tower divided into a number of sections having the same pressure and (b) Free standing beam inflated by an air compressor.

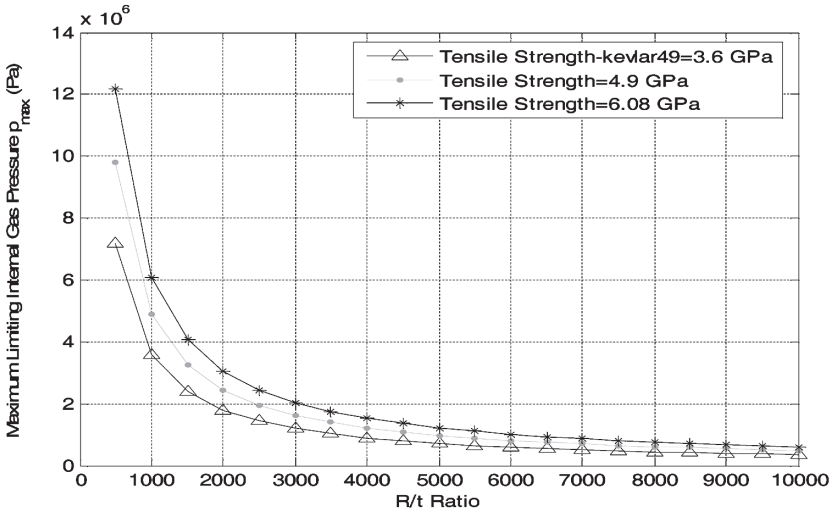

Fig. 4 Maximum limiting gas pressure at various *R*/*t* ratios using different materials.

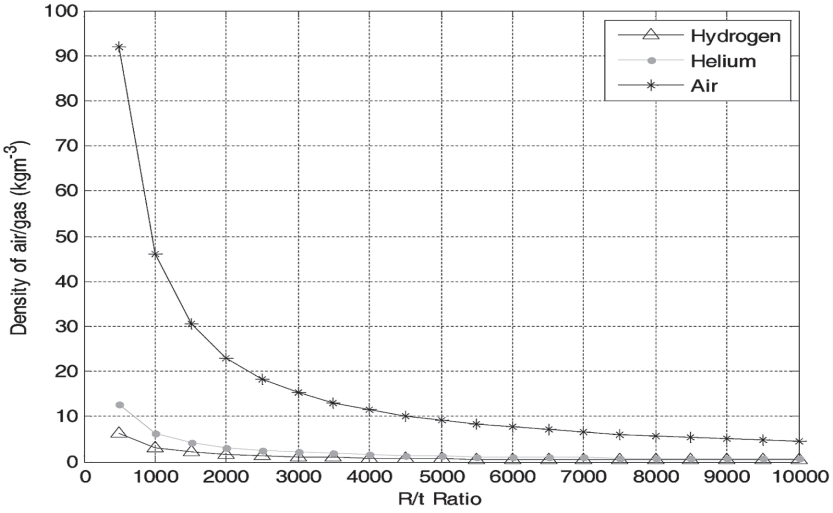

Fig. 5 Variation of gas density with *R*/*t* ratio using Kevlar 49(ρ = 1440 *kg*/*m*^{3}).

$$\rho'_g = \frac{\mu\sigma}{R_g T(R/t)} \quad \text{or} \quad \frac{R}{t}\rho'_g = \frac{\mu\sigma}{R_g T} \tag{9}$$

The quantity

$$\frac{R}{t}\rho'_g$$

measured in kg/m^3, in Eq. (9) is constant for a particular material and for a particular gas to be used. By using Eq. (9) in Eq. (8), the maximum attainable height is also given by

$$H_{\max} = \frac{\sigma}{2\rho g + \left(\frac{\mu\sigma}{R_g T}\right) g} \tag{10}$$

For hydrogen, helium and air inflatable space towers made of Kevlar 49 (σ = 3.6 *GPa*, ρ = 1440 *kg*/*m*^{3}), the maximum attainable height for all *R*/*t* ratios is found to be *57 km*, *37 km* and *7 km* respectively.

The payload capacity per unit cross-sectional area of the inflated tower for particular *R*/*t* ratio, density ρ'_g of air/or gas and the height *H* is given by

$$W'_{payload\_capacity} = p' - \left[\left(\frac{2H\rho g}{R/t}\right) + H\rho'_g g\right] \tag{11}$$

with the condition that $p' \le p_{\max}$.

To calculate maximum payload capacity of the tower of height *H*, for a given *R*/*t* ratio, the value of pressure $p'\left(p' = p_{\max}\right)$ corresponding to its maximum limit is given in Eq. (3). The maximum payload capacity per unit cross-sectional area is then expressed as

$$W'_{\max\_payload\_capacity} = \left[\frac{\sigma}{R/t}\right] - \left[\left(\frac{2H\rho g}{R/t}\right) + H\rho'_g g\right] \tag{12}$$

The maximum load capacities for hydrogen, helium and air towers are computed for the given height at different *R*/*t* ratios, and the results are shown in Fig. 6. Further margin and safety factors can be included following a similar load capacity analysis.

The payload capacity of the tower based on the internal pressure is numerically equal to the tension in the walls. To provide stability for the tower, the tension in the wall should be sufficiently large after placing the payload. The load on the tower contributes to the compressive stress in the walls; however, the wall of the tower should always be under tension instead of compression. Therefore, the weight W_{load} of the payload should always be less than the tension in the wall. The tension in the wall after the contribution of the payload is given by

$$T' = \pi R^2 p' - 2\pi RHt\rho g - \pi R^2 H\rho'_g g - W_{load} \tag{13}$$

For $T' \ge 0$, the value of the internal gas pressure with payload should be as follows:

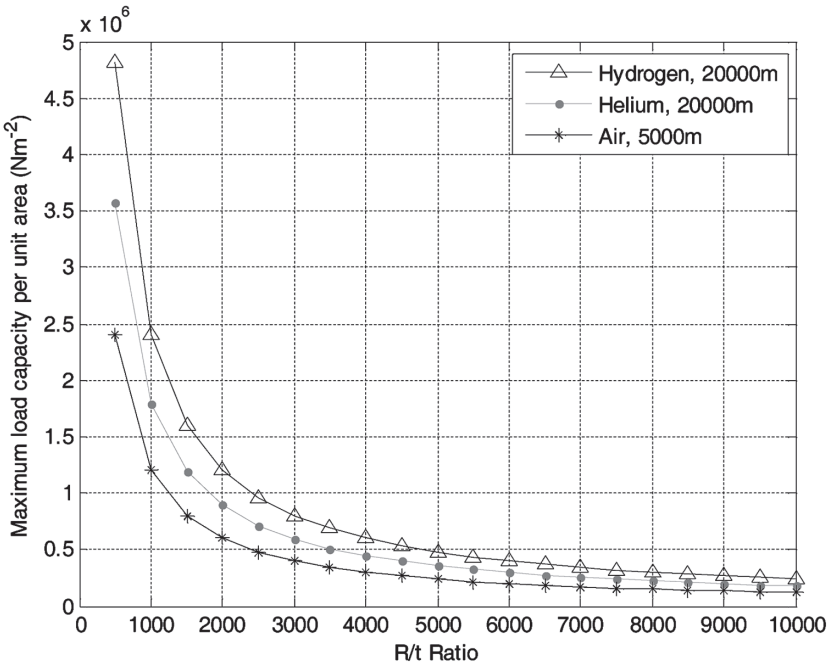

Fig. 6 Maximum load capacity per unit cross-section area for particular tower heights and gases at different *R*/*t* ratios using Kevlar 49 (ρ = 1440 *kg*/*m*^{3}).

$$p' \geq \frac{2H\rho g}{R/t} + H\rho'_g g + \frac{W_{load}}{\pi R^2} \qquad (14)$$

The pressure p' should never exceed $p_{\max}$ for a particular *R*/*t* ratio (see Eq.3).

5.1 Critical Bending Moment

The critical bending moment of the inflated cylindrical beam depends on the critical wrinkling moment of the inflated beam and may be defined as the moment at which the beam wall starts to wrinkle. Below the wrinkling moment limit, the inflated beam can be modelled by Euler beam theory. The developments in the mechanics of inflatable cylindrical beams started in the early 1960s. Leonard *et al* [18] and Comer and Levy [19] studied inflatable cylindrical cantilevered beams using Euler beam theory and derived the values of the wrinkle moment ($M_w = 0.5\pi p'R^3$) and the collapse moment ($M_c = \pi p'R^3$) theoretically. An experimental investigation of inflatable cylindrical cantilevered fabric beams has been conducted in order to obtain design guidelines for the inflated structures. The authors [20] and previous experimental findings from Yoo *et al*. [21] show that the inflatable beam, either highly or lightly inflated, can be modelled by the simple Euler beam theory accurately before the wrinkling occurs. The load-deflection relationships are also linear when the lateral load applied does not exceed a particular limit. It is interesting to note that all the linear parts of load-deflection curves of different inflation pressure have the same slope. This indicates that the unwrinkled inflatable beams are suitably modelled with the Euler beam theory. The slope change of load-deflection curve gives the critical point of wrinkle of the inflated beam.

The authors have previously developed dimensionless load-deflection data from experiments. The inflatable beams made of different materials and sizes can be examined by using the dimensionless form of the load-deflection ratio as an analytical tool. The experimental investigation of the inflated cantilever beam shows that the dimensionless load–deflection between the load *m*

$$(m = \frac{FL}{\pi p' R^3} ,$$

where *F* is the lateral tip load applied at the free end of an inflatable beam having length *L* and radius *R*) and the deflection δ

$$(\delta = \frac{Etd}{p'L^2} ,$$

where *E*, *t* and *d* are the elasticity of the material, thickness and transverse tip deflection of the beam) is approximately linear if the bending moment is less than 0.4, i.e. $m \leq 0.4$ and the shape of the beam is maintained in the linear region [20].

The value of the critical wrinkling moment is given by

$$M_w = m\pi p'R^3 = 0.4\pi p'R^3 \qquad (15)$$

Setting

$$p' = p_{\max} = \frac{\sigma}{R/t}$$

from Eq. (3), the value of the critical bending moment for an inflated beam and hence for the tower can be computed for different values of radii at different inflated pressures and hence for different *R*/*t* ratios as

$$M_w = \frac{0.4\pi\sigma R^3}{R/t} \qquad (16)$$

The result of the computation for the given *R*/*t* ratio at different radii is shown in Fig. 7.

5.2 Bending Moments due to Wind Loads

Wind loads are the dominant critical dynamic loads acting on the structure. These loads vary in intensity depending on the building's geographic location, structural height and shape. Wind is a phenomenon of great complexity and can apply loads to structures from unexpected directions because of the many flow situations arising from the interaction of wind with structure and topology. Some structures, particularly those that are tall or slender, for example bridges,

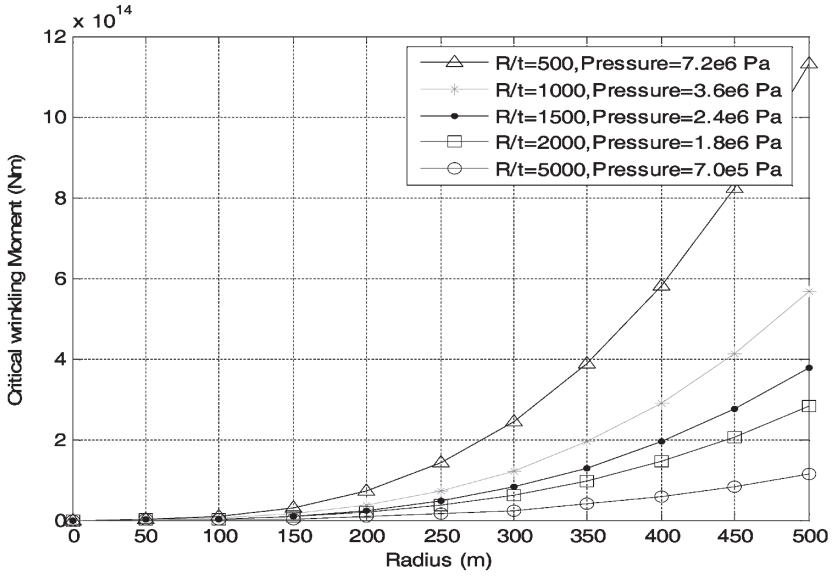

Fig. 7 Variation of critical wrinkling bending moment at various pressures corresponding to different *R*/*t* ratios using Kevlar 49.

respond dynamically to the effects of wind. The best known structural collapse due to wind was the Tacoma Narrows Bridge which occurred in 1940 at a wind speed of only about 19 m/s. It collapsed due to the wind induced vibration resonating in coupled torsional and flexural modes [22]. To minimize the wind load affects, the most suitable geographic location for the space elevator tower structure is the equator, which offers an excellent location on scientific grounds for a high-altitude astronomical observing stations. Located at or near the equator, hurricanes and cyclones occurring within 10 degrees of the equator are nearly absent [23].

The wind load exerting a drag force acting on the structure is given by [24]

$$F_d = \frac{1}{2} C_d \rho_f v^2 .S \tag{17}$$

where ρ_f is the air density, v is the airflow velocity, S is the surface area projected to the airflow (also known as the body frontal area), and C_d is the drag coefficient, respectively.

The value of C_d is a dimensionless number that depends upon the Reynolds number, air turbulence, air viscosity, surface roughness and shape of the structure. For cylindrical shape typically $C_d = 1.2$ [24]. The density ρ_f of air decreases with altitude [17].

Wind velocity v is also not constant, but varies with altitude in a very complex manner which is difficult to predict. The equatorial location of the structure under consideration has its wind speed profile with altitude determined by the Equatorial Atmospheric Radar (EAR) [25, 26], which can be used in computations. Zonal winds are much stronger than the meridional and vertical winds.

The body frontal area for the cylindrical surface is $S = l * D$, where l is length of the cylindrical surface on which air strikes and D is its diameter as shown in Fig. 8. The bending moment at the base of the structure resulting from the wind load acting on a cylindrical section of length l of the tower is given by

$$M_{wind} = F_d .z \tag{18}$$

where z is the vertical distance (height) from ground to the line of action of force F_d as shown in Fig. 8. Substituting Eq. (17) into above equation leads to the wind load moment

$$M_{wind} = \frac{1}{2} C_d \rho_f v^2 S.z \tag{19}$$

Since the values of density of air and wind velocity are functions of altitude z. Therefore, the total moment due to the wind load acting along the entire length of the tower can be calculated by integrating the Eq. (19) from ground $z = 0$ to height $z = h$ such as

$$M_{wind\_total} = \frac{1}{2} C_d . S \int_0^h \rho_f (z).v^2 (z).dz \tag{20}$$

The bending moment due to wind load must be less than the critical wrinkling moment of the inflated beam ($M_w = m.\pi p' R^3$, see Eq. (15)) for the survival of structure, otherwise the structure would start to fail.

Although wind direction is not always perpendicular to the tower, but it is taken to be normal to the surface to evaluate maximum wind load bending moment as shown in the Fig. 9. To evaluate the maximum possible estimated wind load bending moment conservatively, the wind flow is assumed to be in one direction and the tower is divided into four sections (regions) each of length *5000 m*. The average values of wind velocities and atmospheric densities are taken for each section. For estimation of the maximum possible wind load bending moment, all the terms are taken as positive and the total wind load moment is given by the sum of the components.

$$M_{wind\_total} = \sum_i F_{di} .z_i \tag{21}$$

where

$$F_{di} = \frac{1}{2} C_d \rho_{fi} v_i^2 .S$$

is the average force acting on the tower in a particular region at a given altitude. By substitution for the area $S = 2R.l$ and drag coefficient $C_d = 1.2$, the value of the drag force in the *i th* region becomes $F_{di} = C_d \rho_{fi} v_i^2 .R.l$, where subscript i is used for the section or region chosen above the Earth's surface for the respective average values of force, density and velocity in each

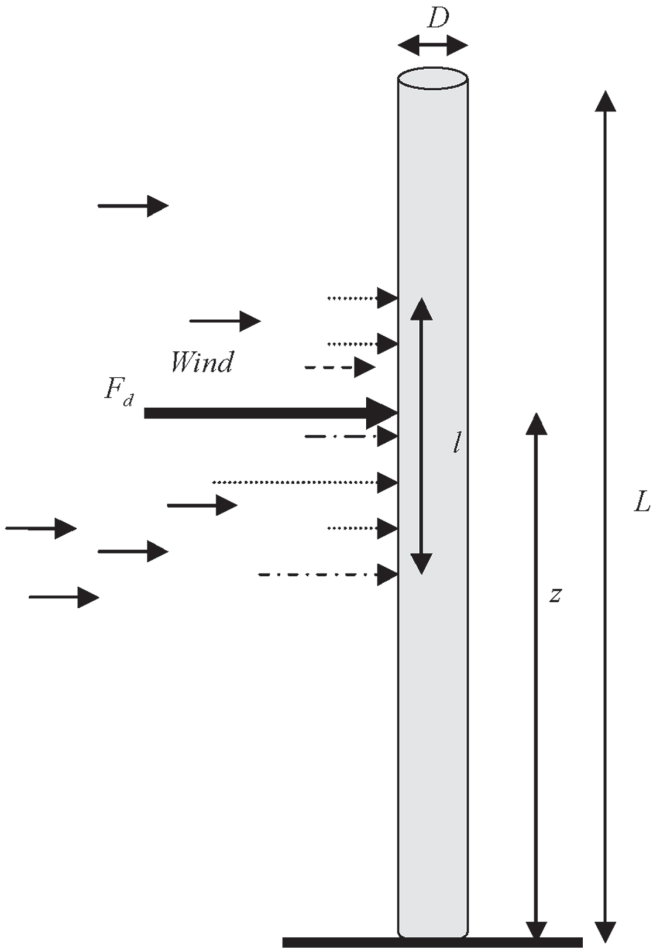

Fig. 8 Cylindrical section of the inflated beam exposed to wind.

region as shown in Fig. 9. The average values of atmospheric density and wind velocity in all the selected four regions along the height of tower are shown in Table 2. The average value of the wind velocity is a maximum in region 3 (10-15 km) and contributes the most in the calculation of the wind load bending moment.

The total wind load bending moment can be written as

$$M_{wind\_total} = 1.2\sum_{i=1}^{4} \rho_{fi} v_i^2 .R.l.z_i$$
$$= 1.2Rl(\rho_{f_1} v_1^2 z_1 + \rho_{f_2} v_2^2 z_2 + \rho_{f_3} v_3^2 z_3 + \rho_{f_4} v_4^2 z_4) \quad (22)$$

The maximum possible bending moment due to the wind load for different radii is estimated by using recent (2007) zonal wind velocity profile data measured by the EAR [26]. The result for different tower heights of using Eq. (22) is also shown in Fig. 10. Pearson anticipates a peak wind velocity of 150 ms^{-1} giving a typical dynamic pressure of 8300 Nm^{-2} applied over a 3 km vertical interval [4]. For a 15 km structure located at a 5 km altitude (e.g. a mountain top at or near the equator), this corresponds to a total dynamic pressure force of 3.0 x 10^9 N applied at approximately 1.5 km above the structure's base [7]. The result of the computation for a 15 km tower having a diameter of 230 m shows that a typical wind dynamic force is approximately 1.5 x 10^8 N, which is 1/20th of the worse case anticipated load value of 3.0 x 10^9 N. By contrast, the Coriolis force ($\vec{F}_c = -2m_p(\vec{\Omega}\times\vec{v}_p)$, $\vec{\Omega}$ be the angular spin rate

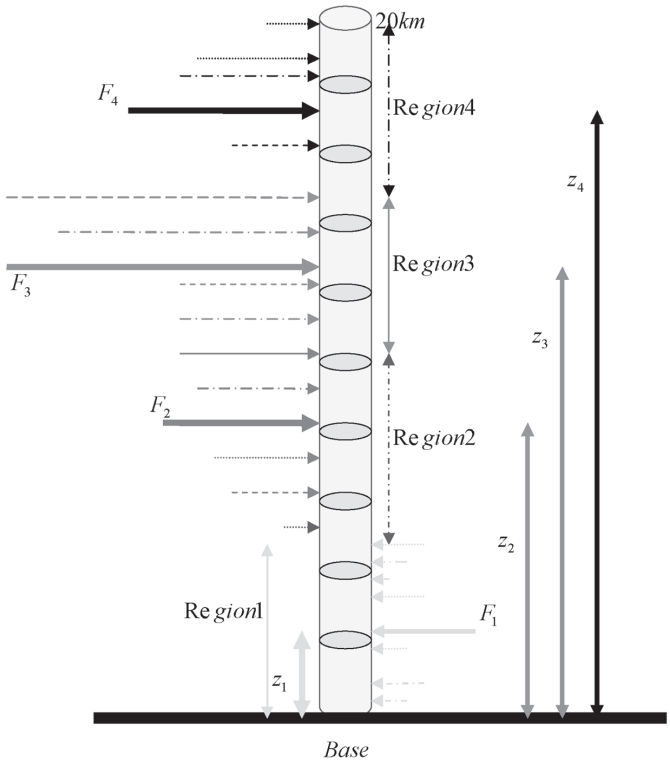

Fig. 9 A 20 km inflatable single beam tower under different wind loads in various regions.

TABLE 2: *Average Wind Velocity and Atmospheric Density.*

Region	Range (km)	Average wind velocity (m/s)	Average atmospheric density(kg/m^3)
1	0 - 5	5.5	0.9
2	5 – 10	6.5	0.54
3	10 – 15	25	0.28
4	15 – 20	12	0.11

of Earth), for example, acting on an elevator capsule carrying payloads weighing 100,000 kg (m_p), moving away from the equator with a velocity of 40 km/h (v_p) is estimated to be 160 N and is negligible and therefore can be neglected in comparison to wind loads while evaluating the lateral tip deflection of the tower.

The lateral tip deflection of the tower due to wind load can be calculated using the following formula [27]:

$$d = \frac{F_d z^2}{6EI}(3L - z), \quad (23)$$

where F_d is the transverse force acting at a distance z from the fixed end (the ground), L is the length of tower (see Fig. 8), and I is the inertia moment of cross section area of cylindrical tower of radius R and thickness t and is formulated as $I = \pi R^3 t$ [27]. Substituting $I = \pi R^3 t$ into Eq. (23) leads to the lateral deflection as

$$d = \frac{F_d z^2}{6\pi R^3 Et}(3L - z). \quad (24)$$

The lateral tip displacement of tower of length L is found by summing the deflections caused by individual transverse loads by using Eq. (24) as

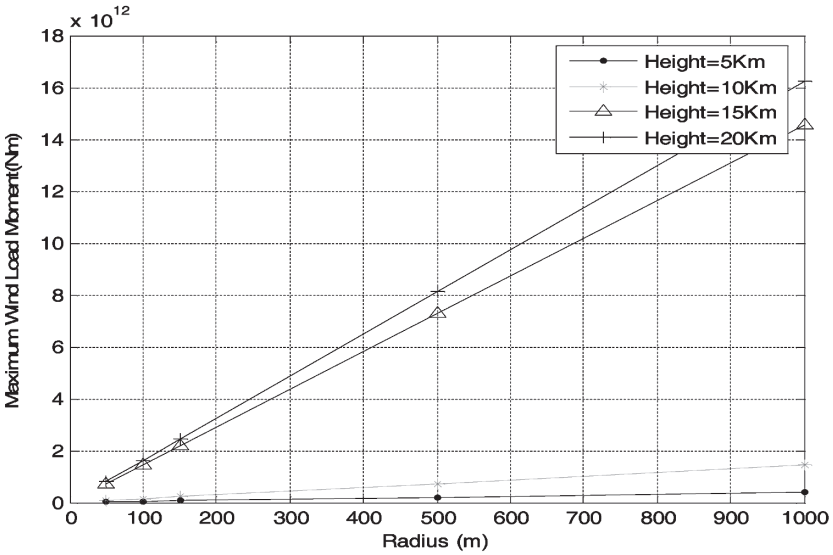

Fig. 10 Wind load variation with tower radius for different heights.

$$d_{total} = \sum_{i}^{4} d_i = \sum_{i}^{4} \frac{F_{d_i} z_i^2}{6\pi R^3 Et}(3L - z_i)$$

Substituting $F_{di} = C_d \rho_{fi} v_i^2 .R.l$ into the above equation, the tip displacement of the tower is given by

$$d_{total} = \sum_{i=1}^{4} \frac{C_d . \rho_{f_i} . v_i^2 . l . z_i^2}{6\pi R^2 Et}(3L - z_i) \qquad (25)$$

The angle of inclination (degrees) or the angle through which the tower deviates is given by

$$\theta = \left[\tan^{-1}\left(\frac{d_{total}}{L}\right)\right]\left(\frac{180}{\pi}\right) \qquad (26)$$

The lateral tip displacement and the angle of inclination due to the wind load are computed for different heights and radii by using Eqs. (25) and (26) and the results of computations for wall thickness *t = 0.1m* are shown in Figs. 11(a) and 11(b). For the towers of *5 km* and *10 km* height, having a radius 50 m, the lateral tip displacement is found to be *20 m* (with angle of inclination 0.23°) and *326 m* (with angle of inclination 1.8°) respectively and may be quite controllable. For *15 km* and *20 km* tower heights having a radius *150 m*, the lateral displacement is *1000 m* (with angle of inclination 3.8°) and *1700 m* (with angle of inclination 4.8°). It is obvious from the computations that the towers of height *15 km* and *20 km* with thickness *0.1 m* and radii more than *150 m* can be controlled because the lateral tip displacement (angle of inclination) decreases with an increase in radius.

5.3 Bending Moments due to Dead Load Contribution of the Tower

Live wind loads cause lateral movement of the tower and during the lateral movement, the bending moment due to the dead load of the tower comes into effect. The dead load of the tower is numerically equal to its weight, which further depends upon the height of the tower, the nature of the material and internal gas pressurization used in the tower. The bending moment due to the dead load depends upon the lean angle and height of the centre of gravity with respect to the Earth's surface. The tower is considered to be highly stable if the lateral movement of the tower under wind load is close to zero. For this reason, the best results obtained in the analysis correspond to the minimum values of the lateral tip displacement under the wind load for given values of tower radius and thickness of the cover material for a particular tower height.

The damping effect may be achieved actively using a high pressure line-and-vent network system and passively by allowing the support gas to vent from compartment to compartment along a connecting line network. For the primary bending moment the force component exerted perpendicular to the core structure is *mg* sin θ. Therefore, for a building lean angle of 1.0°, the component force is 1/57th of the tower weight. The reaction force could be applied by making use of active control mechanisms to stabilize the structure [7].

6. INFLATED MULTI-BEAM STRUCTURE

The lateral movement of the tower is undesirable as it exasperates the dead load contribution of the tower. For this reason, the control of a single beam inflatable tower is only possible if the tower radius is sufficiently large. Due to this reason, an inflatable multiple-beam structure is highly recommended because the structure can be actively controlled by the differential change of internal gas pressure in the inflatable beams. Moreover, multiple-beam structure can be designed easily for zero tip displacement using inflatable beams of certain radii and separated symmetrically from each other.

The stability and control issue of the inflated tower can be solved by using a multiple inflated beam structure. This is illustrated in Fig. 12 and Fig. 2 with a structure consisting of three inflated beams. The number of beams can be increased as required. The inflated beams are braced intermittently to stabilize the multi-beam structure and their spacing is optimized for the collapse moment and the buckling strength of the inflated beams. The bending moments can be actively controlled by changing the pressure in each beam. The wrinkling bending moment depends upon the applied pressure *p*, the number of inflated beams *N*, the radius of each inflated beam *R* and the radius *r* of the structure as illustrated in Fig. 12. The inflated multi-beam structure was designed in the laboratory and deployed in a stairwell (Fig. 2). The brackets are designed to hold the inflated beams and the vertical space through the centre of the structure can be used for carrying the payloads as shown in Fig. 13.

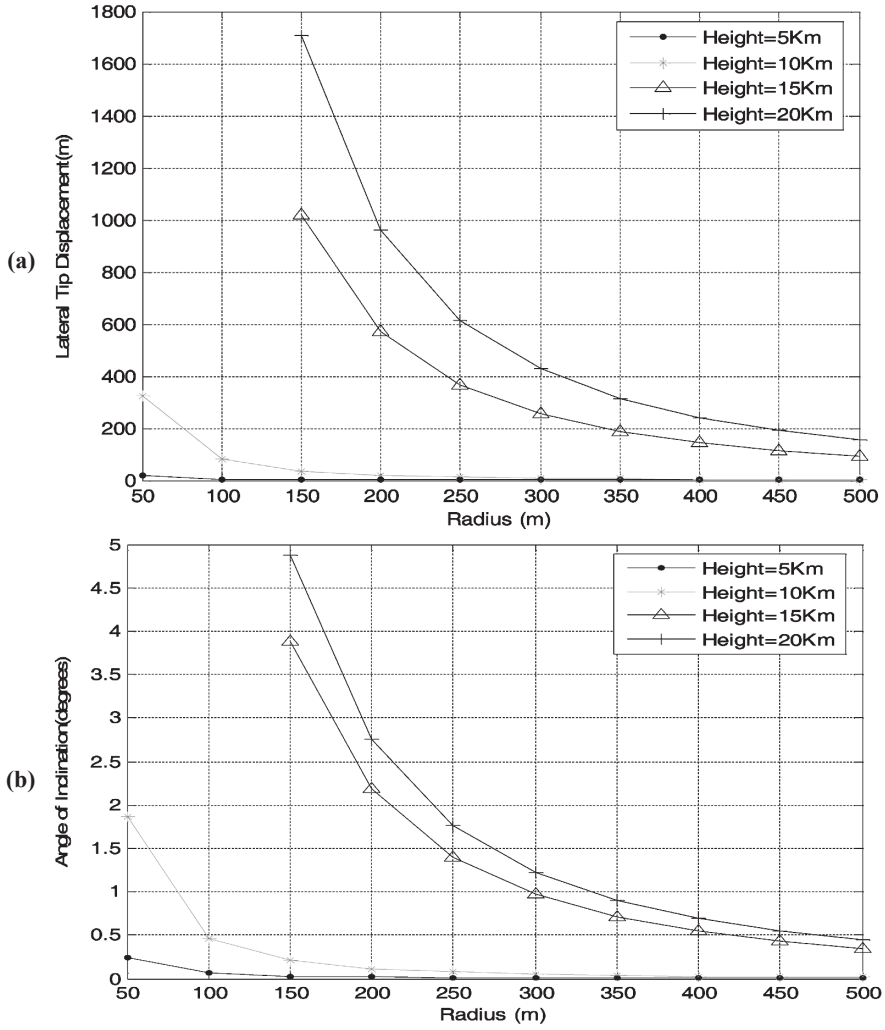

Fig. 11 (a) Variation of lateral tip displacement of the tower at different heights and thickness *0.1 m* and (b) Variation of angle of inclination of the tower of different heights and thickness *0.1 m*.

The moment of inertia of the cross sectional area of the multiple-beam structure about any arbitrary axis passing through the centre *O* (e.g. the axes *OX*, *OY* and *OX*') is found to be same. The three beams *A*, *B* and *C*, each having radii *R* are equidistant from each other and centred at the circumference of the circle of radius *r*, such that *AB* = *BC* = *CA* as shown in Fig. 12. The inertia moment of the cross sectional area of the structure about the *OX*-axis is given by

$$I_x = \pi R^3 t + 2\pi R t r^2 + 2\left[\pi R^3 t + 2\pi R t\left(\frac{r}{2}\right)^2\right] = 3\pi R t\left(R^2 + r^2\right)$$

The area moment of inertia about *OY*-axis is also given as

$$I_y = \pi R^3 t + 2\left[\pi R^3 t + 2\pi R t\left(r\cos 30^0\right)^2\right] \quad = 3\pi R t\left(R^2 + r^2\right) \tag{27}$$

This indicates that the inertia moment of the cross sectional area is independent of the axis used.

It is also found that in the case of a multi-beam structure consisting of 4, 5, 6…*N* inflated beams of radius *R*, centred symmetrically at the circumference of the circle of radius *r*, the area moment of inertia of the configuration about any axis passing through the centre of the circle in its plane of cross-section is directly proportional to N, the number of inflated beams in the multi-beam structure.

Therefore, Eq. (27) can be generalized for *N* number of beams and can be written as

$$I = N\left[\pi R t\left(R^2 + r^2\right)\right] \tag{28}$$

The flexural rigidity *EI* (Nm^2) of the inflated multi-beam structure is given by

$$(EI)_{multi} = NE\pi R t\left(R^2 + r^2\right) \tag{29}$$

The composite beam equation for the inflated multiple-beam structure with the introduction of pressure p' becomes

$$\frac{FL}{N\pi p' R\left(R^2 + r^2\right)} = \frac{3Etd}{p' L^2} \tag{30}$$

The critical dimensionless load m' for the multiple beam structure consisting of *N* inflated beams can be stated as

$$m' = \frac{FL}{N\pi p' R(R^2 + r^2)} \tag{31}$$

The critical bending moment for the inflated multi-beam structure is given by

$$M_{w\_multi} = m' N\pi p' R\left(R^2 + r^2\right) \tag{32}$$

Substituting

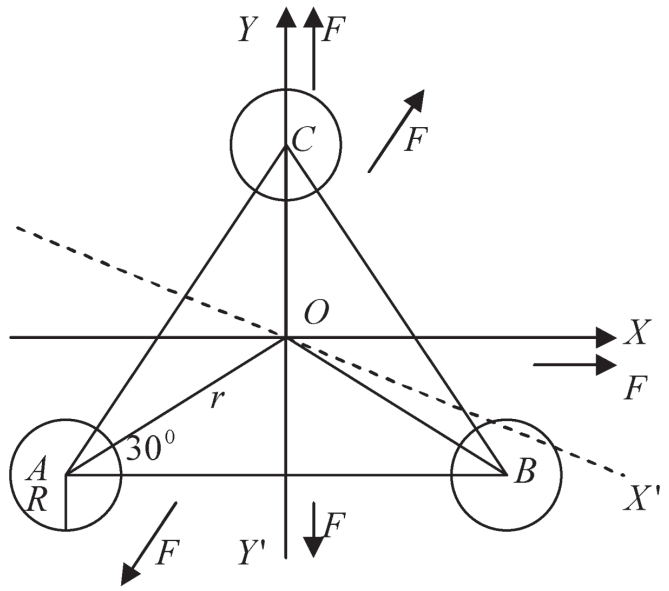

Fig. 12 Multi - beam structure cross section consisting of three inflated beams.

$$p' = p_{\max} = \frac{\sigma}{R/t}$$

into Eq. (32), the critical bending moment of the inflated multiple-beam structure for the given material and R/t ratios can be computed by using the following relationship

$$M_{w\_multi} = m'N\pi R^3 \left(\frac{\sigma}{R/t}\right)\left(1+\frac{r^2}{R^2}\right) \tag{33}$$

6.1 Comparison of Single Inflated Beam with Inflated Multi-Beam Structure

The inflated multiple-beam structure consisting of N inflated beams inflated with pressure p', can be reduced to a single inflated beam equivalent by taking into account the respective critical bending moments by using Eqs (15) and (32).

$$\frac{M_{w\_multi}}{M_w} = \frac{m'NR\left(R^2+r^2\right)}{mR^3} \tag{34}$$

The above equation can be written as

$$\frac{M_{w\_multi}}{M_w} = \frac{m'}{m}N\left(1+\frac{r^2}{R^2}\right) = K.M_w$$

$$K = \frac{m'}{m}N\left(1+\frac{r^2}{R^2}\right) \tag{35}$$

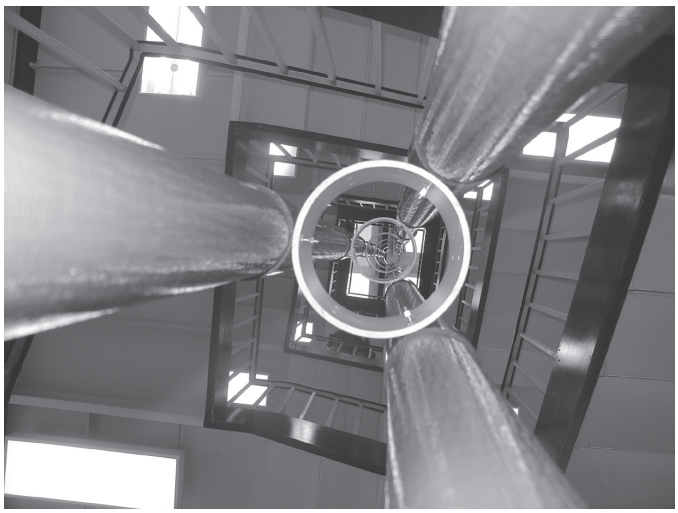

Fig. 13 The vertical space through the centre of inflated multi-beam structure.

where K is a factor, which depends upon the structure parameters. Therefore, the critical value of the bending moment for the inflated multi-beam structure is K times the critical bending moment of the single inflated beam and inflated multi-beam structures can be designed as required, by choosing suitable values of the parameters involved in Eq. (35) to overcome the wind load. As the number of beams separated by certain distance is increased, the wind load also increases and can be estimated separately for each structure.

7. CONCLUSION

The theory and computation presented here shows the feasibility of an inflatable space tower constructed from Kevlar 49. It has been found that towers of height 5-10 km can be controlled if the radius is above 50 m. Space towers of height 15 km to 20 km require a radius of at least 150 m. The primary reason for instability is the wind load in tower region 3 (10-15 km altitude), which contributes the most due to the high wind speed. The stability and control factors can potentially be increased by using multiple-beam structures. The stability of a multiple-beam structure depends upon the geometry (radius of each beam and the interspacing between the beams) of the structure in addition to the internal gas pressure. The attitude of the inflated multi-beam structure can also be guided actively by differential changes of pressure in the inflated columns. The tower can be utilized as a platform for various scientific and space missions or as an elevator to carry payloads and tourists. Suborbital towers will also likely be required for the construction of a geosynchronous space tether as they would provide an ideal surface mounting point where the orbital tether could be attached without experiencing the atmospheric turbulence and weathering in the lower atmosphere.

REFERENCES

1. M. Lou, and V. Feria, "Development of Space Inflatable/Rigidizable Structures Technology", *Proceedings of IUTAM-IASS Symposium on deployable structures – Theory and Applications*, Cambridge, U.K., September 1998.
2. D.V. Smitheman Jr., "Space Elevators", NASA/CP-2000-210429, 2000.
3. K.E. Tsiolkovski, "*Speculations About Earth And Sky on Vesta*", Moscow, Academy of Sciences, U.S.S.R., Moscow, p.35, 1999.
4. J. Pearson, "The orbital tower: a spacecraft launcher using Earth's rotational energy", *Acta Astronautica*, **2**, pp.785-799, 1975.
5. A. C. Clarke, "*Fountains of Paradise*", Harcourt Brace Jovanovich, New York, 1978.
6. A.A. Bolonkin, "Optimal Inflatable Space Towers with 3-100km Height", *JBIS*, **56**, pp.87-97, 2003.
7. B.M. Quine, R.K. Seth and Z.H. Zhu, "A free standing space elevator structure: A practical alternative to the space tether", *Acta Astronautica*, **65**, pp.365-375, 2009.
8. R.E. Freeland, S. Bard, G.R. Veal, G. Bilyeu, C. Cassapakis, T. Campbell and M.C. Bailey, "Inflatable antenna technology with preliminary shuttle

experiment results and potential applications", Washington: CP96-1367, AIAA, Washington, DC, 1996.
9. R.E. Freeland and G.R. Veal, "Significance of the inflatable antenna experiment technology", Washington: CP98-2104, AIAA, Washington, DC,1998b.
10. D. Tanner, J. Fitzgerald, D. R. Phillips, "The Kevlar Story – an Advanced Materials Case Study", *Angewandte Chemie International Edition*, **28**, pp. 649–654, 1989.
11. "Standard Test Method for Tensile Properties of Glass Fiber Strands, Yarns, and Rovings Used in Reinforced Plastics", D 2343, Annual Book of ASTM Standards, ASTM.
12. "Standard Methods of Testing Tire Cords, Tire Cord Fabrics, and Industrial Filament Yarns Made from Man-Made Organic-Base Fibers", D 885, Annual Book of ASTM Standards, ASTM .
13. E.E. Magat, "Fibres from Extended Chain Aromatic Polyamides", *Philos. Trans. R. Soc., (London) A*, **294**, pp.463-472, 1980.
14. B.C. Edwards, "The space elevator: NIAC phase I report" 2001, B.C. Edwards, "The space elevator: NIAC phase II final report", 2003.
15. P.K. Aravind, "The Physics of the Space Elevator", *Am. J. Phys*, **75**, pp.125-130, 2007.
16. Warren C. Young and Richard Budynas, "*Roark's Formulas for Stress and Strain*", The McGraw Hill Companies, 2001.
17. Properties Of The U.S. Standard Atmosphere 1976, "Public Domain Aeronautical Software", P.O. Box 1438 Santa Cruz CA 95061 USA.
18. R.W. Leonard, G.W. Brooks and H.G. McComb Jr., "Structural considerations of inflatable re-entry vehicles", NASA TN D-457, Virginia, USA, 1960.
19. R.L. Comer and S. Levy, "Deflections of inflated circular cylindrical cantilever beam", *AIAA J.*, **1**, pp.1652-1655, 1963.
20. Z.H. Zhu, R.K. Seth and B.M. Quine, "Experimental Investigation of Inflatable Cylindrical Cantilevered Beams", *JP Journal of Solids and Structures*, **2**, pp.95-110, 2008.
21. E.J. Yoo, J.H. Roh and J.H. Han, "Wrinkling control of inflatable booms using shape memory alloy wires", *Smart Mater. Struct.*, **16**, pp.340-348, 2007.
22. P. Mendis, T. Ngo, N. Haritos, A. Hira, B. Samali, J. Cheung, "Wind Loading on Tall Buildings", *EJSE Special Issue: Loading on Structures*, pp.41-54, 2007.
23. Robert A. Fesena, "A high-altitude, station-keeping astronomical platform", Submitted on 15 Jun 2006. http://arxiv.org/abs/astro-ph/0606383.
24. Theodore A. Talay, "Introduction to the Aerodynamics of Flight", SP-367, NASA, Washington, D.C. 1975.
25. Schoichiro Fukao, Hiroyuki Hashiguchi, Mamoru Yamamoto, Toshitaka Tsuda, Takuji Nakamura, and Massayuki K. Yamamoto, "Equatorial Atmosphere Radar (EAR): System description and first results", *Radio Science*, **38**, 1053, doi:10.1029/2002RS002767, 2003.
26. Equatorial Atmosphere Radar (EAR) Observation Data (version 02.0212) provided by research institute for sustainable Humanosphere of Kyoto University.
27. James M. Gore, "*Mechanics of materials, sixth edition*", A division of Thomson Learning Inc., 2006.

(Received 17 December 2008; 7 April 2010)

* * *